Journal of Applied Research in Water and Wastewater
E-ISSN: 2476-6283
Journal homepage: https://arww.razi.ac.ir

Synthesis of magnetic nanoparticles (Fe_3O_4) coated with fatty acids and surfactants and their application in demulsification of crude oil and water emulsions

Farhatsadat Meibodi*, Ebrahim Soori

Department of Organic Chemistry, Faculty of Chemistry, Razi University, Kermanshah, Iran.

GRAPHICAL ABSTRACT

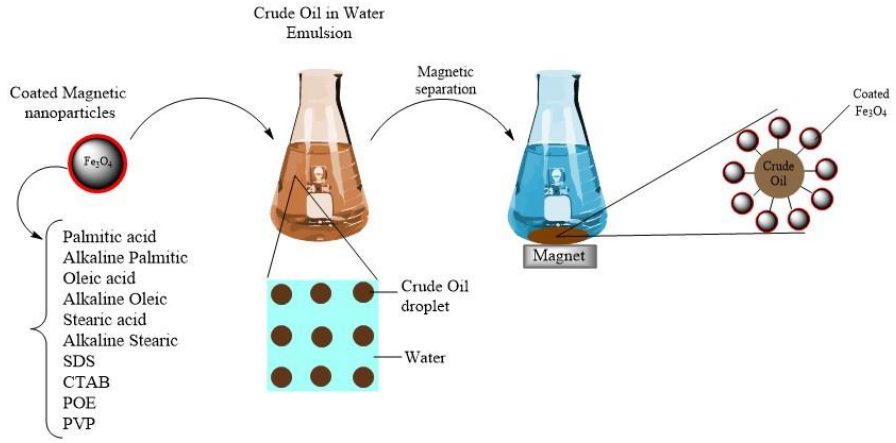

ARTICLE INFO

Article type:
Research Article

Article history:
Received 25 January 2023
Received in revised form 26 April 2023
Accepted 29 April 2023
Available online 2 May 2023

Keywords:
Magnetic nanoparticles
Emulsification
Demulsification
Water and crude oil emulsion
Fatty acids
Surfactants

ABSTRACT

Crude oil is released into the water sources during exploration, extraction or displacement operations due to the partial dissolution, and it can remain as a layer on the surface of the water or become emulsive. Crude oil emulsion is very stable due to the presence of asphaltene and cannot be removed by the common methods. In this research, iron oxide nanoparticles were coated with oleic acid (OA), stearic acid (SA), sodium dodecyl sulfate (SDS), cetyltrimethylammonium bromide (CTAB), polyvinylpyrrolidone (PVP) and polyoxyethylene (POE), by using the same method. After synthesizing iron oxide nanoparticles and coating their surface with fatty acids and surfactants, we have tried to break the crude oil emulsion in water and remove the crude oil from the environment by adsorption via these nanoparticles. Fourier transform infrared spectroscopy (FT-IR), transmission electron microscope (TEM), scanning electron microscope (SEM), thermal gravimetric analysis (TGA), vibration sample magnetometer (VSM), energy-dispersive X-ray spectroscopy (EDS), X-ray diffraction (XRD) and Zeta potential devices were used to identify nanoparticles and their characteristics. Demulsification of crude oil in water (O/W) with nanoparticles coated with fatty acids and surfactants was studied. UV-Vis spectrophotometery was used to determine the amount of crude oil adsorption by nanoparticles. From the results, the nanoparticles coated with the fatty acids with smaller chains could more absorb the crude oil. The highest adsorption (98.03 %) was recorded for iron oxide nanoparticles coated with polyoxyethylene (Fe_3O_4@POE) and the lowest percentage (46.69 %) is related to the nanoparticles coated with palmitic acid in an alkaline medium. Alkalinization of the medium while coating the nanoparticles with fatty acid has increased only the efficiency in the case of oleic acid while led to a significant decrease in the efficiency for palmitic and stearic acids compared to the neutral state.

1. Introduction

Environmental pollution, especially water resources, has increased at an unprecedented rate in recent years, which could lead to the extinction of all living beings on earth. Crude oil is a valuable and essential material for human life; both in terms of energy supply and production of raw materials required by industry. But like everything else, in addition to the many benefits, it has many disadvantages that can seriously endanger the life of living organisms, especially aquatic organisms (M. Alzahrani and Rajendran, 2019). Oil in water causes

*Corresponding author Email: Meibodyf@yahoo.com

Cite this article: F. Meibodi, E. Soori, Synthesis of magnetic nanoparticles (Fe_3O_4) coated with fatty acids and surfactants and their application in demulsification of crude oil-in-water emulsions, *Journal of Applied Research in Water and Wastewater*, 10 (1), 2023, 36-47. https://doi.org/10.22126/arww.2022.6975.1227

depletion of dissolved oxygen due to the transformation of the organic component into inorganic compounds (Onwurah *et al.*, 2007). Toxic compounds in crude oil also have various adverse effects on the environment, such as air pollution due to oil evaporation and the entry of hydrocarbons into the atmosphere. In addition, they can affect groundwater, seawater or drinking water (Han *et al.*, 2019).

In recent years, large amounts of emulsified petroleum and oil wastewater have been produced from the oil and food industries, leading to severe environmental problems. The hydrocarbons found in crude oil spillage are large and complex molecules, so they are highly stable in nature and are not easily destroyed (Essien and John, 2011). Crude oil has 200 to 300 different compositions, very complex mixtures of several thousand hydrocarbons and unspecified additives. About 98-50% of petroleum compounds are related to hydrocarbons, which are mainly alkanes, cycloalkanes, aromatic compounds (20 to 40% crude oil) such as benzene, toluene, xylene, naphthalene, anthracene, phenanthrene, as well as polycyclic compounds such as pyrene. Also, the amount of sulfur compounds, fatty acids, nitrogen compounds, and metals such as iron, titanium, zinc, copper, vanadium, and nickel reach 10% (Chicarelli *et al.*, 1990).

When oil leaks into water, depending on the droplet size, depth, and energy of the system, the droplets may remain dispersed or may mix with other oil droplets to reach the surface. Oil droplets less than 20 microns in diameter can be stably dispersed in water for a long time without coming to the surface (Cui *et al.*, 2020) (Cui et al. 2020).

An emulsion is a highly stable colloidal solution in which the two organic and aqueous phases are dispersed without mixing. Depending on the number of phases, crude oil-in-water (O/W) emulsion, water-in-crude oil (W/O) emulsion, or multilayer emulsions such as water-in-crude oil-in-water (W/O/W) will be formed (Hong *et al.*, 2012; Costa *et al.*, 2019).

Today, nanotechnology has made significant progress in various sciences and industries and has solved many problems by producing more durable, lighter and more economical tools and materials. Using of nanoparticles, especially magnetic nanoparticles due to the high surface-to-volume ratio and having magnetic properties (Issa *et al.*, 2013; Ganapathe *et al.*, 2020), in the adsorption and removal of elements, compounds and contaminants have received much attention (Lu and Astruc, 2018). Magnetic property is one of the properties that are highly dependent on the size of the particle. Therefore, as we move to the nanoscale and the particle shrinks, the surface-to-volume ratio increases and effects on particle's magnetic properties (Akbarzadeh, Samiei and Davaran, 2012).

There are magnetic elements such as iron, cobalt, nickel and their chemical compounds in the structure of magnetic nanoparticles. Although, nickel and cobalt show high magnetic moment but it was predicted to cause toxicity because unlike iron, they are not essential elements in our body and may accumulate in the body and cause various diseases (Jiao *et al.*, 1996; Kafrouni and Savadogo, 2016).

Nanoparticles can be prepared by physical, chemical and biological methods Physical methods include lithography (Colson, Henrist and Cloots, 2013) and gas phase deposition (Grammatikopoulos *et al.*, 2016). Chemical methods include oxidation (Ozkaya *et al.*, 2009), sol-gel (Takai *et al.*, 2019), co-precipitation (Kandpal et al. 2014), electrochemical method (Marín *et al.*, 2016), supercritical fluid method (Adschiri and Yoko, 2018). Biological methods involve the use of microbes (Shamim *et al.*, 2018) Although physical methods are easier, particle size control is difficult in these methods. Wet chemical methods such as sol-gel or co-precipitation can control the particle size by fine-tuning the effective parameters, nanostructured engineering and surface modification (Ali *et al.*, 2016).

Magnetic nanoparticles will tend to aggregate and form a mass due to their very small size and superparamagnetic properties, which reduces the efficiency and performance of these nanoparticles. Modification of nanoparticle surface prevents agglomeration and oxidation as well as improves physicochemical properties and mechanical properties (Zhu *et al.*, 2018). The surface of nanoparticles can be coated with materials such as surfactants, polymers, fatty acids and minerals such as silica (Bagwe, Hilliard and Tan, 2006). Surfactants such as sodium dodecyl sulfate (Han *et al.*, 2016), lauric acid (Mamani *et al.*, 2013), etc., or polymers such as polyethylene glycol (Nunes *et al.*, 2018), polyvinyl alcohol (Salunkhe *et al.*, 2013), and polyvinyl pyrrolidine (Khamis, Hamdy and Morsi, 2018), or natural materials such as gelatin (Mahmoudi Saber, 2019), starch (Masina *et al.*, 2017), chitosan (Yu *et al.*, 2019), dextran (Tassa, Shaw and Weissleder, 2011), and polylactic acid (Nobs *et al.*, 2003) are used to modify the surface of nanoparticles. Carbon (Vidal *et al.*, 2008) or metals such as gold (Ban *et al.*, 2005) or platinum (Park and Cheon, 2001) are also used for this purpose.

Recently, the use of magnetic nanoparticles in various industrial and medical applications such as magnetic storage (Thompson and Best, 2000), catalysis (Wang *et al.*, 2015), electrocatalysis (Garcés-Pineda *et al.*, 2019) targeted drug delivery (Garcés-Pineda *et al.*, 2019), magnetic resonance imaging (MRI) (Arsalani *et al.*, 2019) and cancer treatment through magnetic hyperthermia (Jose *et al.*, 2020) has been considered.

In this work, magnetic iron oxide nanoparticles (Fe_3O_4) were synthesized by the chemical co-precipitation method and were coated with fatty acids such as palmitic acid (PA), oleic acid (OA) and stearic acid (SA) as well as surfactants such as sodium dodecyl sulfate (SDS), cetyltrimethylammonium bromide (CTAB), polyoxyethylene (POE) And Polyvinyl pyrrolidone (PVP). The nanoparticles were coated with fatty acids in both neutral and alkaline media.

By using these nanoparticles, the crude oil in water (O/W) emulsion is broken and the crude oil is trapped and absorbed by the nanoparticles. These nanoparticles are then deposited and separated with a magnet. After demulsification and separation, UV spectra were taken from the solution to determine the amount of crude oil adsorption by nanoparticles.

2. Materials and methods

2.1. Synthesis of Fe_3O_4 nanoparticles

The chemical co-precipitation method was used to synthesize iron oxide nanoparticles. This method is simple, fast and the produced nanoparticles show good quality and acceptable size. In this method, magnetic iron oxide nanoparticles or magnetite were synthesized by two species of Fe^{3+} and Fe^{2+} in a ratio of 2:1 and in an alkaline environment with a pH close to 11. $FeSO_4.7H_2O$ (0.001 mol, 2.78 g) and $FeCl_3$ (0.002 mol, 3.24 g) were dissolved in 100 mL of distilled water. The solution was stirred until it turned a light orange-brown color. The reaction was exothermic. Then 11 mL of ammonia was added dropwise to reach pH 11 and stirred by a magnet on a magnetic stirrer at 60°C in the presence of N_2 gas until the solution turned black and the magnetic nanoparticles were produced. Finally, the nanoparticles were precipitated by a strong magnet and washed several times with water and ethanol and decanted to neutralize the pH. The separated nanoparticles were poured into a crystallizing dish and dried into an oven at 70°C for 24 h.

2.2. Synthesis of modified Fe_3O_4 nanoparticles coated with fatty acids and surfactants

Iron oxide nanoparticles (1 g) in 10 mL of ethanol were dispersed and stirred on a magnetic stirrer at high speed for 10 min. Palmitic acid (0.5 g) was added to it and placed in an ultrasonic bath for 20 min. Finally, it was stirred for 2 h at reflux at 80°C on a high-speed magnetic stirrer. After 2 h, the nanoparticles were separated by a magnet and washed several times with distilled water, and finally dried in an oven at 70°C for 12 h. Iron oxide nanoparticles were coated with OA, SA, SDS, CTAB, PVP and POE, by using the same method (Ong, Suppiah and Muhd Julkapli, 2020).

2.3. Synthesis of Fe_3O_4 nanoparticles modified by palmitic acid, oleic acid and stearic acid in alkaline medium

Iron oxide nanoparticles were coated with palmitic acid (Fe_3O_4@PA) as in the previous method, with the difference that during the reaction, by adding a few drops of ammonia, the pH of the medium is increased to 11. Finally, after coating, the nanoparticles are washed several times with water and ethanol to reach a neutral pH. Similarly, the nanoparticles with OA and SA were modified.

2.4. Preparation of crude oil in water (O/W) emulsion

Crude oil (2.5 mL) was added to 50 mL of distilled water and mixed on a magnetic stirrer at high speed for 5 min, and then sodium dodecyl sulfate (1 g) was added as a surfactant and emulsion stabilizer. Placed in an ultrasonic bath for 10 min and then stirred for 2 h on a magnetic stirrer. After 24 h, the solution was passed through a filter paper to leave only the crude oil that had become an emulsion.

2.5. Demulsification of crude oil in water (O/W) emulsion with nanoparticles coated with palmitic acid

Iron oxide nanoparticles coated with palmitic acid (0.05 g) were added to 5 mL of the prepared crude oil- in-water emulsion and placed into an ultrasonic bath for 10 min to well disperse the nanoparticles. It was then

stirred on a magnetic stirrer for 2 h to absorb the crude oil. After 18 h, placed the solution on the magnet, precipitated the nanoparticles and poured the solution into the test tube to perform UV analysis. This step was performed by nanoparticles coated with OA, SA, SDS, CTAB, PVP and POE, as well as nanoparticles coated in an alkaline medium with PA, OA and SA.

UV visible experiments were performed on samples with different concentrations using a standard solution of 100 mg/L crude oil and in the wavelength range of 200-600 nm. For each sample, the absorbance measurement was repeated three times. The data were plotted as absorbance vs concentration and the maximum absorbance signal was selected for each concentration. Then calibration curves were graphed and the weigh % of the analyzed crude oil was calculated using the calibration curve formula

3. Results and discussion

3.1. Characterization of Fe_3O_4 NPs

FT-IR spectra were used to confirm and characterize the functionalization of nanoparticles. TEM and SEM images were used to determine the morphology and size of the nanoparticles as well as the amount of aggregation. XRD analyses were utilized to characterize the phase and type of nanoparticles, The EDS analysis confirmed the coating of magnetite nanoparticles and specified the percentage of elements in the sample, VSM determined the magnetic strength of the nanoparticles, TGA thermograms were also used to investigate the behavior of nanoparticles at high temperatures and to characterize the weight percentage of the organic layer and Zeta potential was used to measure the electric charge on the surface of magnetic nanoparticles and aggregation. The amount of crude oil absorbed by the nanoparticles was investigated using the UV spectrum

3.1.1. FT-IR

The FT-IR spectra of magnetite nanoparticles coated with fatty acids in both neutral and alkaline media are shown in Fig. 1. Hydrogen bonds and hydroxyl groups on the surface of the nanoparticles are located at 3416 cm^{-1} and 1622 cm^{-1}, respectively. Asymmetric and symmetric stretching of CH_2 group was observed at 2922 cm^{-1} and 2852 cm^{-1}. Stretching of the COO^- group appears at 1405 cm^{-1}. The peak of 1084 cm^{-1} is related to the stretching vibration of the single CO bond, which indicates the chemical adsorption of fatty acids on the nanoparticles, and the peak of 633.56 cm^{-1} is related to the Fe-O bond. Stretching vibration of the double bond in oleic acid was observed at 2103 cm^{-1}.

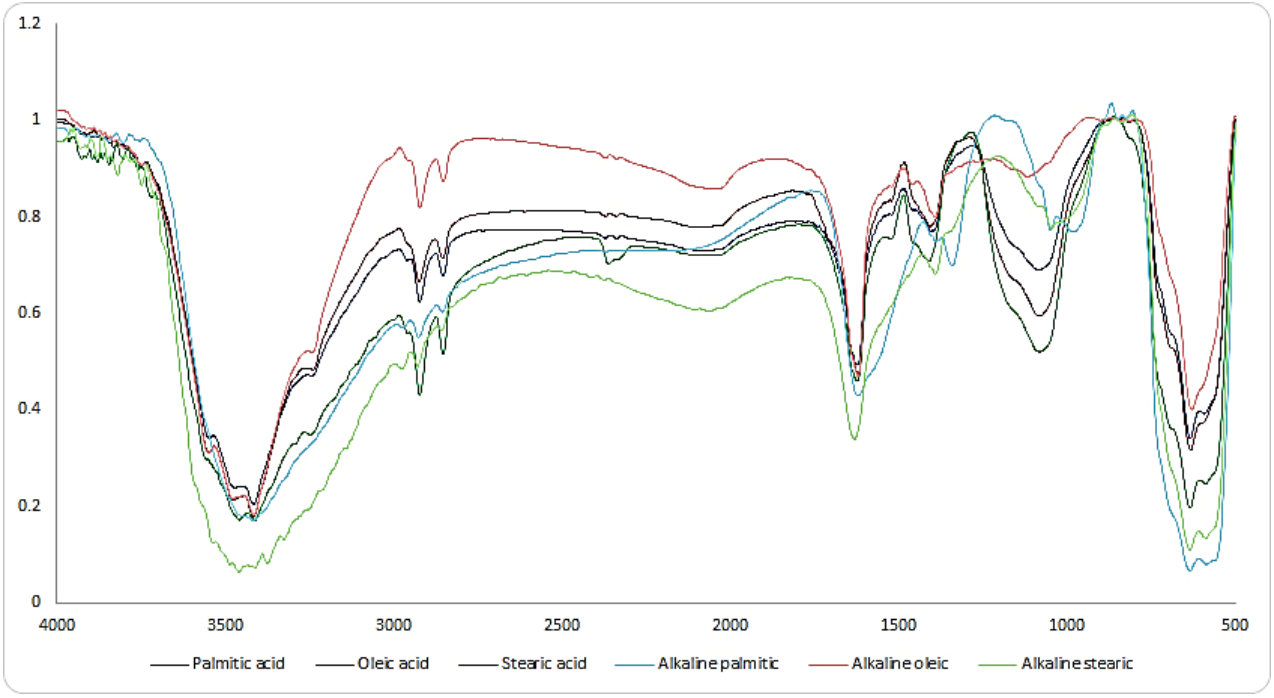

Fig. 1. FT-IR spectrum of magnetite nanoparticles coated with fatty acids in both neutral and alkaline media.

Fig. 2 shows the FT-IR spectra of nanoparticles with surfactants coating; (a) Fe_3O_4@SDS, (b) Fe_3O_4@CTAB, (c) Fe_3O_4@POE and (d) Fe_3O_4@PVP spectrum. In spectrum (a) Fe-O bond vibrations were observed at 630 cm^{-1} and 585 cm^{-1}. Peak of 1134 cm^{-1} was assigned to double bond S=O, peak 1392 cm^{-1} was related to S-O bond. The asymmetric (CH_2) and symmetric (CH_2) stretching vibrational frequencies are located at 2924 and 2854 cm^{-1}, respectively. Hydrogen bonding and OH bonds on nanoparticles appeared at 3417 cm^{-1}. In spectrum (b); the ($N–CH_3$) and *ν*(C–N) are observed at 1388 and 977 cm^{-1}, respectively, which is in good agreement with the data in the literature (Venkataraman and Vasudevan, 2001) In spectrum (c); the stretching vibration of the C-O-C bond was observed at 839 cm^{-1}, the vibration of the O-CH_2 bond has appeared at 1392 cm^{-1}, and the peak of 2923 cm^{-1} is related to the presence of CH_2 in the polymer composition. In spectrum (d); peak 588 cm^{-1} belongs to the Fe-O bond, peak 1126 cm^{-1} is related to the stearic C-O bond, peak 1737.86 is related to the stretching vibrations of the C=C bond, peak 1290 cm^{-1} belongs to the CN bond, peak C=O polymer appears at 1641 cm^{-1}. Peaks at 2924 cm^{-1} and 2852 cm^{-1} are related to polymer carbon chain and 3124 cm^{-1} are related to hydrogen bonds with nitrogen.

3.1.2. TEM images

Transmission electron microscopy of iron oxide nanoparticles coated with palmitic acid, oleic acid and SDS are shown in Fig. 3. The TEM images indicated that the prepared nanoparticles are generally spherical and have uniform nanosize distribution, with an average size of 10 to 40 nm, but are mostly in the range below 20 nm. In the case of palmitic acid, adhesion and aggregation are very low and a large distance was observed between the nanoparticles, which mean that it is properly covered by an organic layer, but in the case of SDS, a little agglomeration is observed, and it is much more in oleic acid. Due to the presence of the organic layer on the surface of nanoparticles, repulsion is created between them. This layer also reduces the magnetic strength of the nanoparticles, which reduces aggregation and also prevents oxidation.

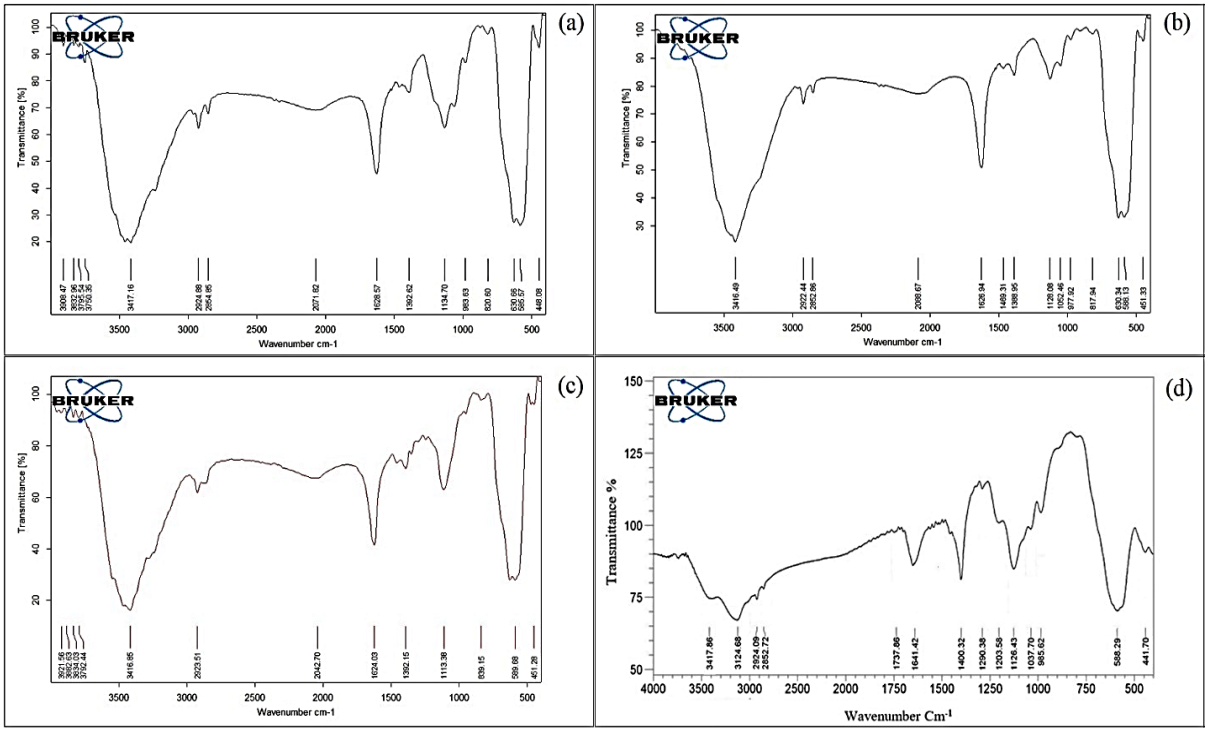

Fig. 2. FT-IR spectra of nanoparticles with surfactants coating; (a) is related to Fe_3O_4@SDS, (b) is related to Fe_3O_4@CTAB, (c) is related to Fe_3O_4@POE and (d) is related to Fe_3O_4@PVP spectrum.

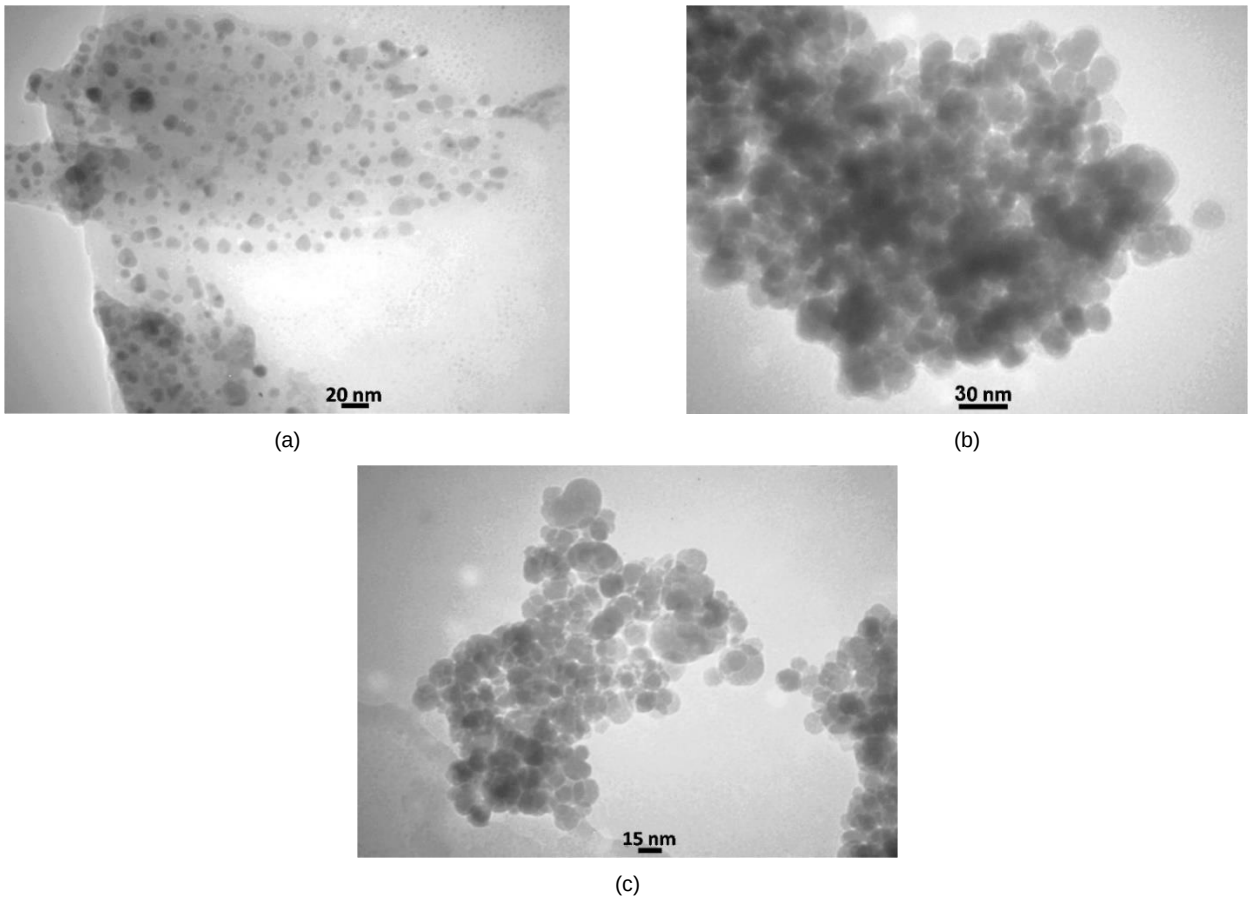

(a) (b)

(c)

Fig. 3. Transmission electron microscopy (TEM) of iron oxide nanoparticles coated with (a) palmitic acid (b) oleic acid and (c) SDS.

3.1.3. SEM image

The scanning electron microscope (SEM) images of iron oxide nanoparticles are shown in Fig. 4. These images show that the nanoparticles are generally amorphous or spherical. The nanoparticles coated with palmitic acid and CTAB are not agglomerated, but the nanoparticles coated with POE are highly cohesive. These images also show that the size of the nanoparticles is generally below 50 nm.

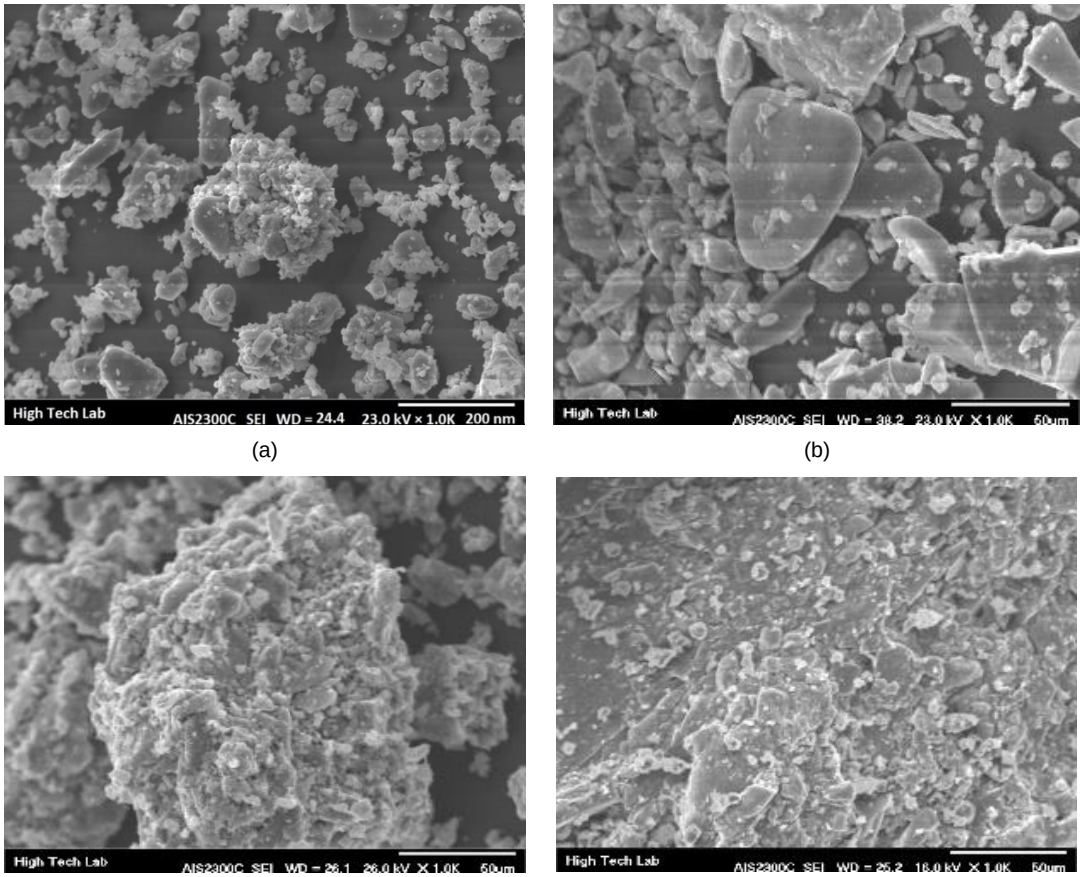

Fig. 3. Scanning electron microscope (SEM) images of iron oxide nanoparticles (a) Fe_3O_4@CTAB, (b) Fe_3O_4@PA, (c) Fe_3O_4@POE and (d) Fe_3O_4@SDS.

3.1.4. XRD analysis

XRD analyses of coated iron oxide nanoparticles are shown in Fig. 5. Index peaks at 2θ=18.40, 30.27, 35.65, 43.34, 57.33, 62.96 indices (111) (220) (311) (400) (511) and (440) for magnetite nanoparticles coated with palmitic acid and oleic acid, respectively, are specified. For nanoparticles coated with SDS and CTAB little difference in 2θ that occurred as 2θ= 18.36, 30.22, 35.60, 43.26, 57.22, 62.84. According to the pattern conformed to these analyzes by Xpert software, the nanoparticles have a cubic structure with reference code 96-900-5841. Also, the peak intensities in the XRD pattern of Fe_3O_4@CTAB nanoparticles are higher than the others and then nanoparticles coated by palmitic acid and oleic acid, and finally, nanoparticles coated with SDS has the lowest intensity, respectively.

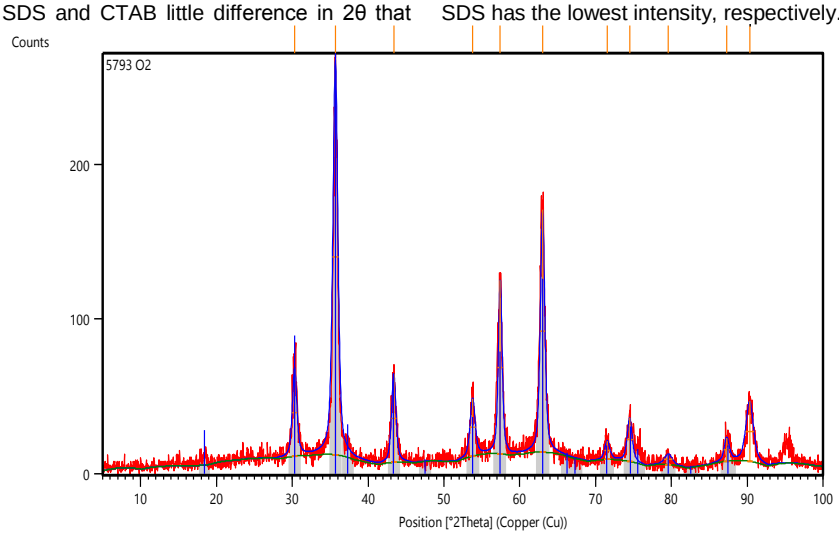

(a)

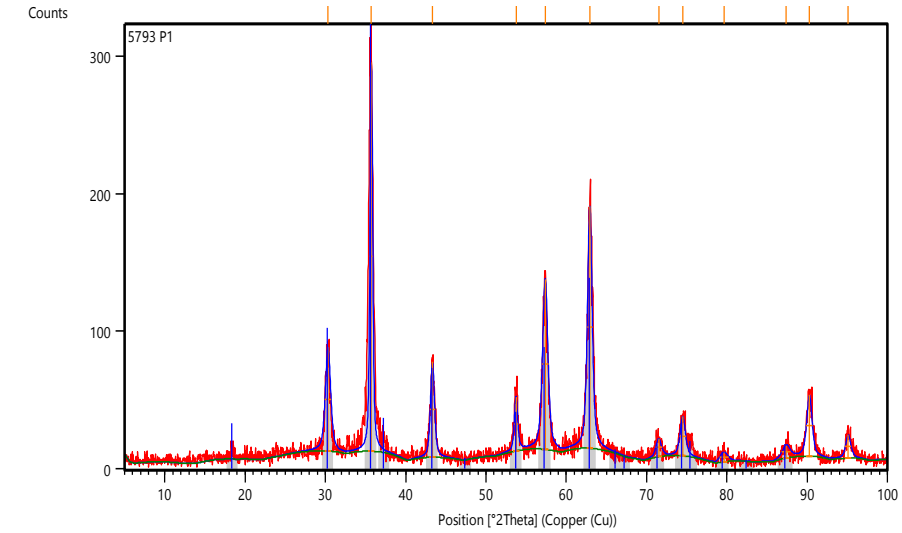

(b)

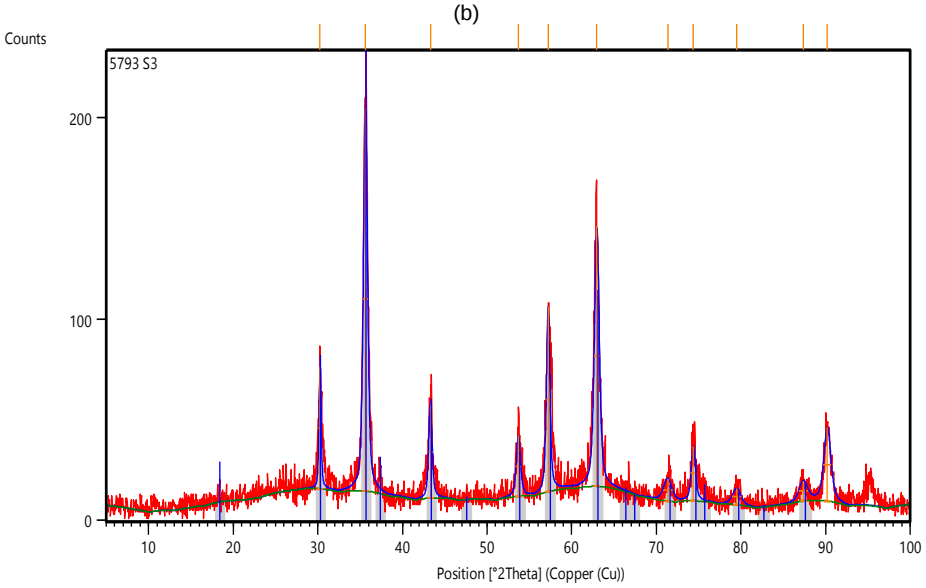

(c)

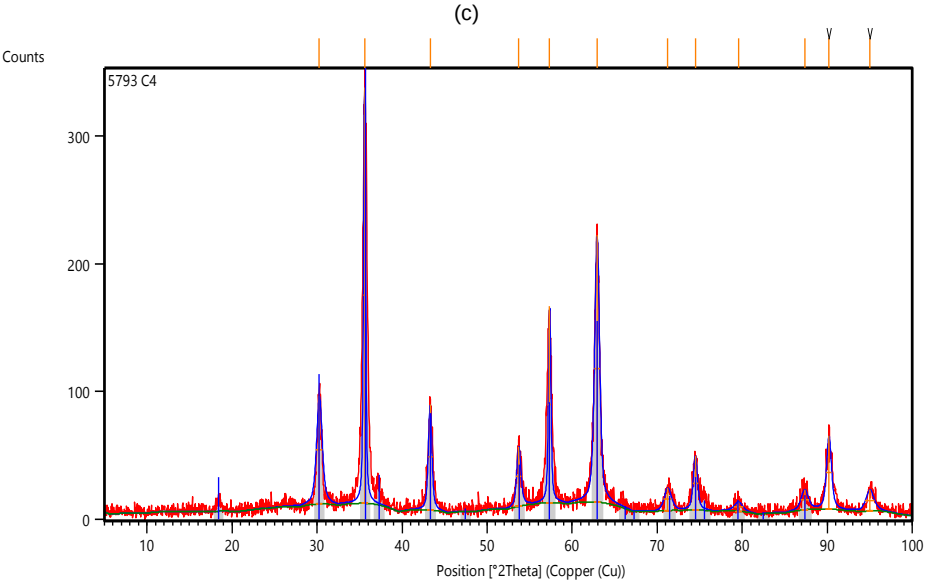

(d)

Fig. 4. XRD pattern of coated iron oxide nanoparticles; (a) Fe_3O_4@Palmitic acid, (b) Fe_3O_4@Oleic acid, (c) Fe_3O_4@SDS, (d) Fe_3O_4@CTAB.

3.1.5. EDS Spectroscopy

Fig. 6a is the energy-dispersive X-ray Spectroscopy (EDS) spectrum of Fe_3O_4@PA nanoparticles. This image shows that the sample consists of three elements: iron, carbon and oxygen; and shows that the nanoparticle is coated with palmitic acid. The highest peak in the spectrum and the maximal weight percentage are related to oxygen. Figure 6b is the EDS spectrum of Fe_3O_4@CTAB nanoparticles. In this sample, the highest weight percentage is related to iron and oxygen, which is because the weight of the organic layer is much less than the

weight of nanoparticles. The presence of nitrogen, bromine and carbon elements confirms the coating of nanoparticles with CTAB.

The EDS spectrum of Fe_3O_4@POE nanoparticles is shown in Fig. 6c. In this sample, iron and oxygen are the most abundant elements. Because polymer polyethylene or polyethylene glycol is made only of carbon, oxygen and hydrogen, the presence of carbon and oxygen indicates the successful coating of nanoparticles by polyoxyethylene. Hydrogen due to its lightness did not appear in the spectrum. The EDS spectrum of Fe_3O_4@SDS nanoparticles is shown in Fig. 6d. In this spectrum, iron and oxygen are the most abundant and the presence of sulfur and sodium elements indicates the success of coating iron oxide nanoparticles with sodium dodecyl sulfate.

3.1.6. VSM analysis

The vibration sample magnetometer (VSM) analysis diagram of four different samples is shown in Fig. 7. The magnetic strength of iron oxide nanoparticles was measured after coating with PA, OA, SDS and CTAB. As it turns out, iron oxide nanoparticles coated with SDS and CTAB have reduced the magnetic strength of the nanoparticles slightly, possibly due to the thin layer around the nanoparticles, but nanoparticles that coated with fatty acids, especially oleic acid, further reduce the magnetic strength of the nanoparticles. This is because oleic acid has 18 carbons and palmitic acid has 16 carbons and forms a thicker coating around the nanoparticles.

3.1.7. TGA analysis

In thermal gravimetric analysis (TGA), the samples were kept at 40°C for one minute and then heated at 30°C /min until the temperature reached 700°C. The first mass loss observed in the samples occurred at 100 to 200°C, which is related to the loss of moisture absorbed (Fig 8). Table 1 shows the information for each sample.

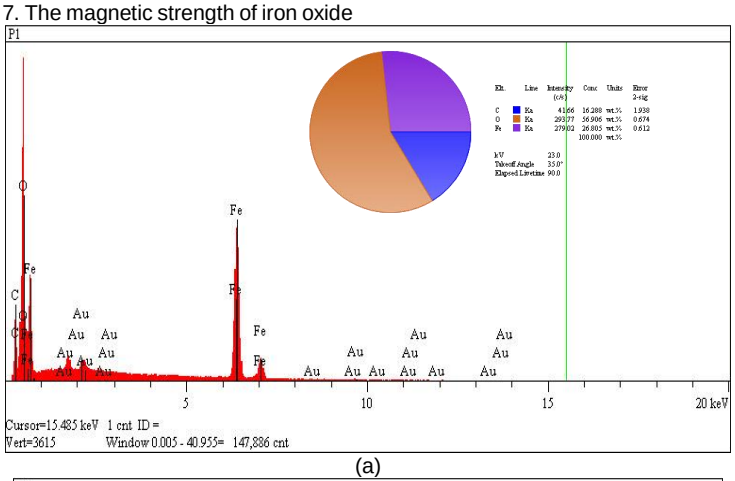

(a)

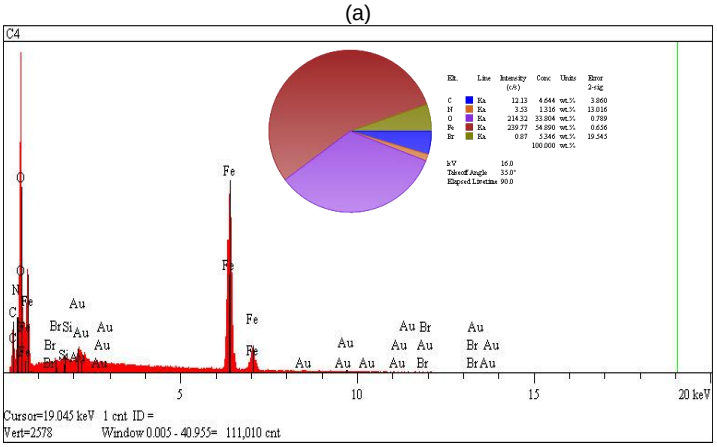

(b)

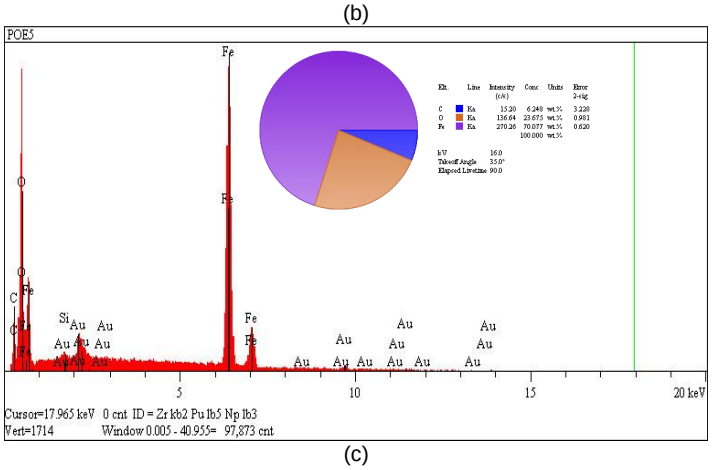

(c)

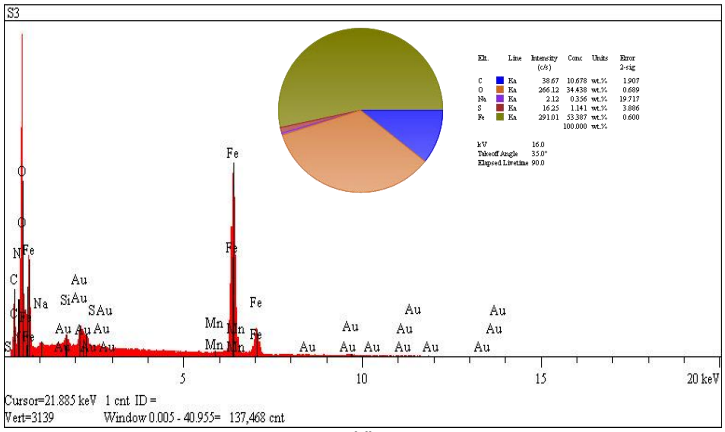

(d)

Fig. 5. Energy-dispersive X-ray Spectroscopy (EDS) spectrum; (a) Fe_3O_4@PA, (b) Fe_3O_4@CTAB, (c) Fe_3O_4@POE, (d) Fe_3O_4@SDS.

Table 1. Information of TGA for each sample.

Samples	Temperature range	Weight loss, %	Total sample weight	Organic layer weight
Fe_3O_4@PA	250-500	6.5	21.03	1.36
Fe_3O_4@OA	200-600	8.0	8.67	0.69
Fe_3O_4@SDS	200-600	7.8	36.94	2.88
Fe_3O_4@CTAB	210-600	6.8	26.11	1.77

3.1.8. Zeta potential analysis

Since the actual surface charge density cannot be measured a relative term namely the zeta potential is measured. The particle zeta potential is a crucial physical property of nanoparticles. Zeta potential was used to measure the electric charge on the surface of magnetic nanoparticles (Fig. 9). The results showed that the surface charge of Fe_3O_4@Palmitic acid nanoparticle is -44.75 mV and Fe_3O_4@Stearic acid is -26.1 mV. Magnetic iron oxide nanoparticles (Fe_3O_4) have a negative charge. Because the number of carbon atoms of stearic acid is higher than palmitic acid, it has reduced the negative charge on the surface of nanoparticles of Fe_3O_4@Stearic acid compared to Fe_3O_4@Palmitic acid. Solutions with zeta potential above +20 mV or below −20 mV are considered stable (Cosgrove, 2009). An increase in surface charge density indicates decreased tendency for aggregation (Prathna *et al.*, 2011) due to electrostatic repulsion.

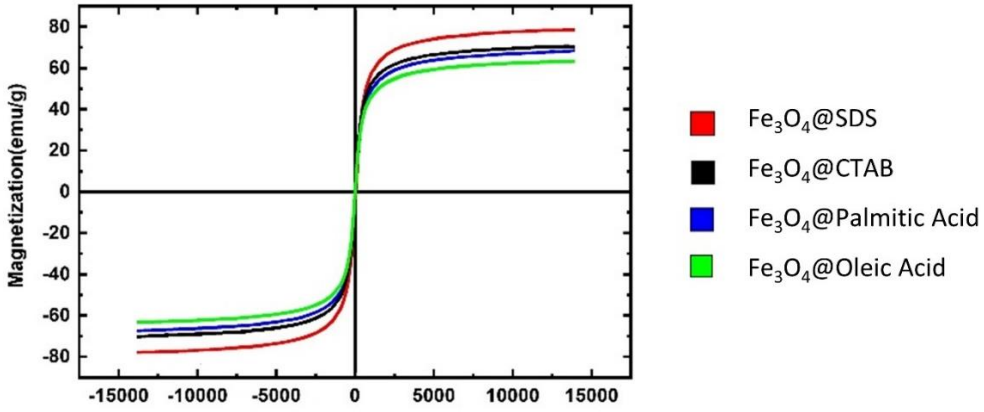

Fig. 6. Vibration sample magnetometer (VSM) analysis diagram.

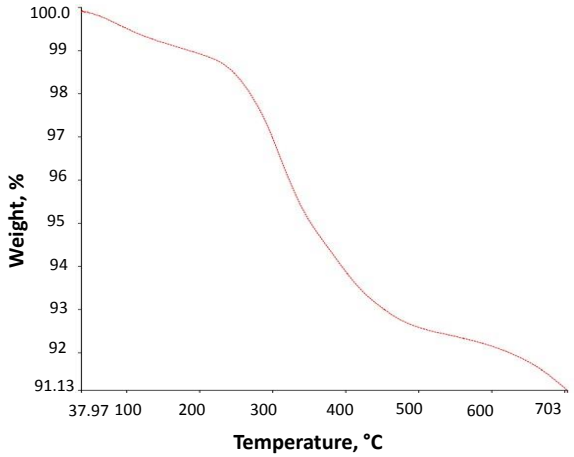

(a)

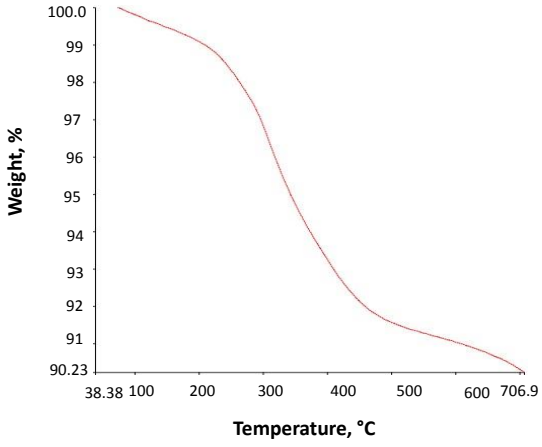

(b)

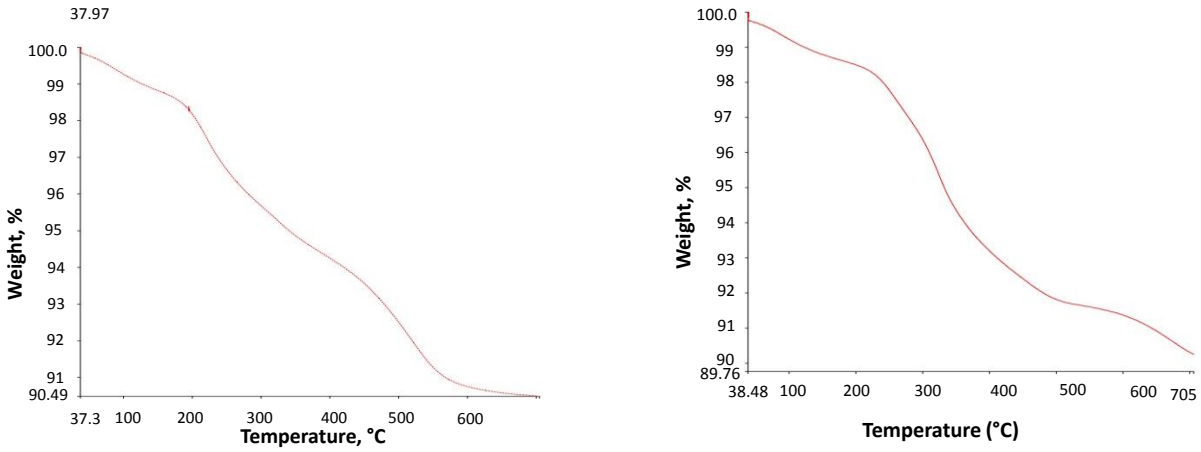

(c) (d)

Fig. 7. Thermal gravimetric analysis (TGA) thermogram; (a) Fe_3O_4@palmitic acid, (b) Fe_3O_4@oleic acid, (c) Fe_3O_4@SDS, (d) Fe_3O_4@CTAB.

3.2. Demulsification of crude oil in water (O/W) emulsion with nanoparticles coated with fatty acids and surfactants

Iron oxide nanoparticles coated with PA, OA, SA, SDS, CTAB, PVP and POE, as well as nanoparticles coated in alkaline medium with PA, OA and SA were added to the prepared crude oil- in-water emulsion and placed into an ultrasonic bath to well disperse the nanoparticles. It was then stirred on a magnetic stirrer for 2 h to absorb the crude oil. After 18 h, placed the solution on the magnet, precipitated the nanoparticles and poured the solution into the test tube to perform UV analysis.

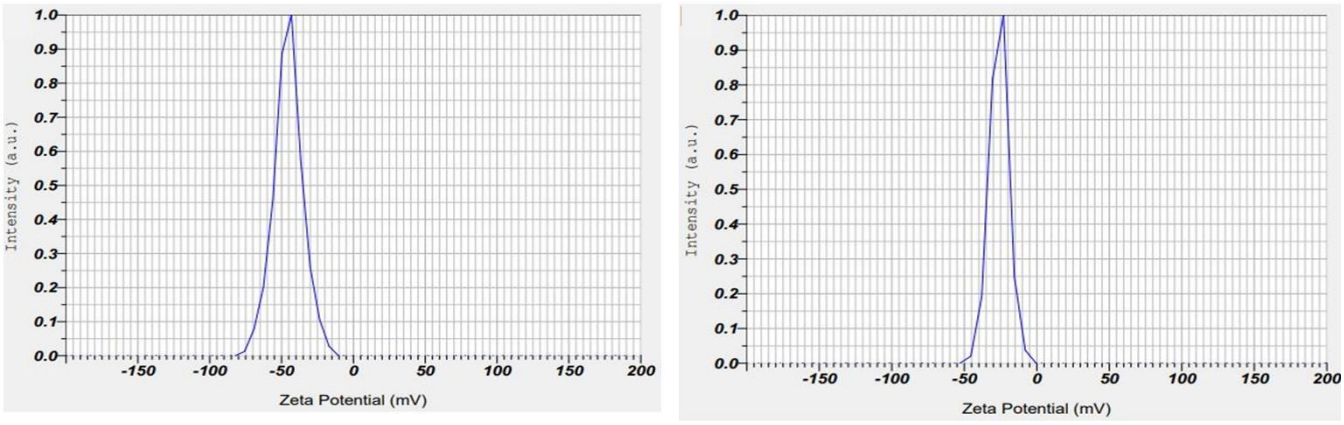

(a) (b)

Fig. 9. The zeta potential diagram of a) Fe_3O_4@Palmitic acid and b) Fe_3O_4@Stearic acid.

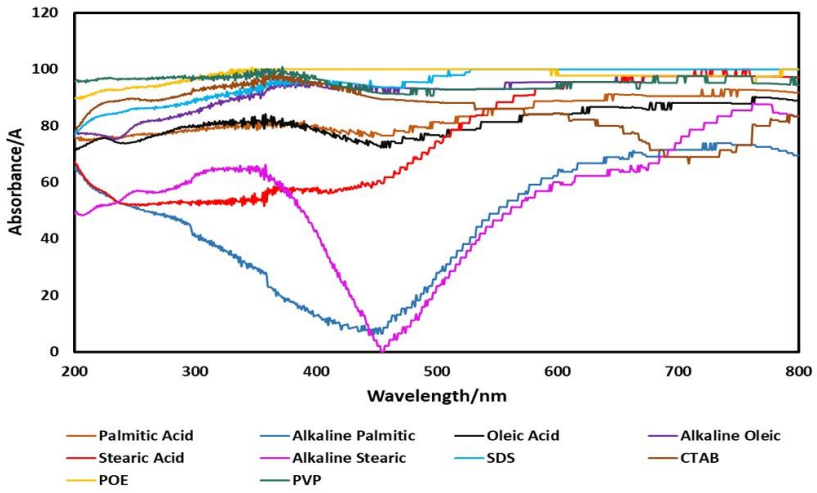

Fig. 10. Relative percentage of absorption of crude oil by nanoparticles in terms of wavelength.

3.2.1 UV-Vis Spectroscopy

Fig. 11 shows the UV-Vis spectra of crude oil-in-water emulsion separation (demulsification). The black line is the spectrum of crude oil-in-water emulsions before separation, and as it turns out, in the range of 450 to 200 nm, nanoparticles coated with PVP and POE had the highest amount of crude oil adsorption. Iron oxide nanoparticles coated with PA and SA in both neutral and alkaline media had the lowest adsorption. The relative percentage of absorption of crude oil by nanoparticles in terms of wavelength is shown in Fig. 11.

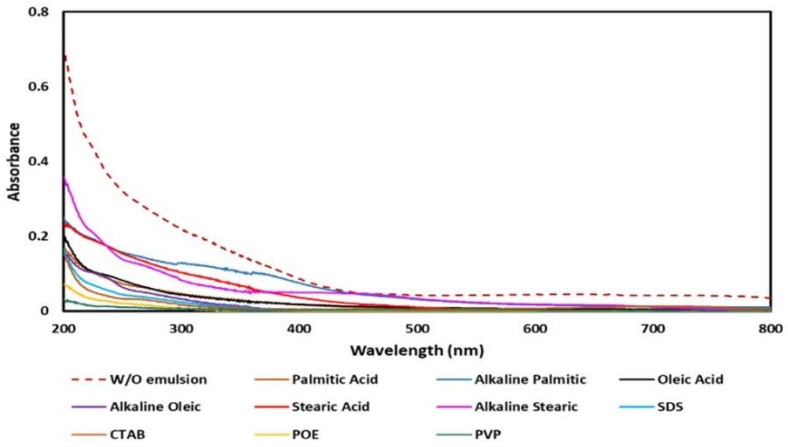

Fig. 11. UV-Vis spectra of crude oil-in-water emulsion separation.

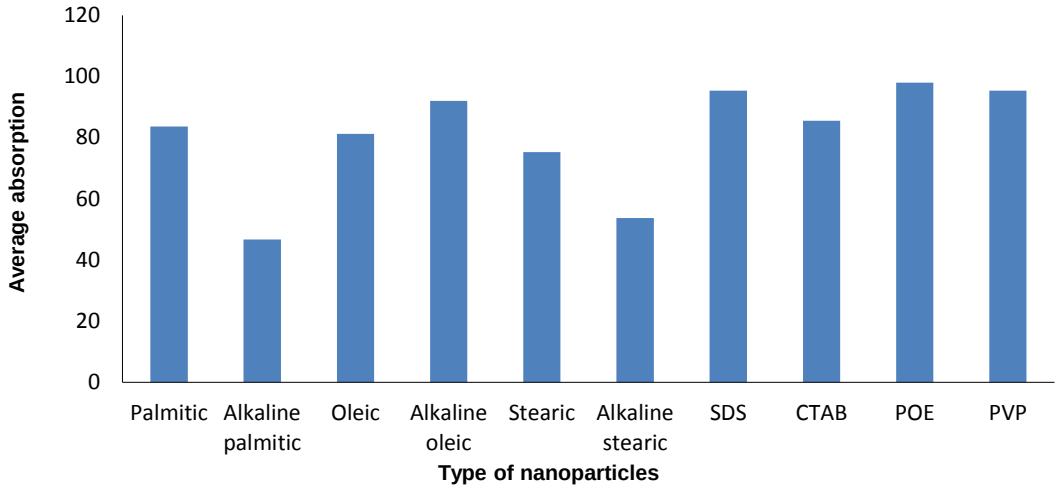

Fig. 12. Average absorption of nanoparticles in the region of 800 to 200 nm.

Nanoparticles which were coated by PVP, POE and SDS showed high adsorption and were constant at almost all wavelengths; but nanoparticles were coated with palmitic acid and stearic acid in alkaline media showed low adsorption and a sharp decrease in near-zero at the range of 400 to 500 nm. Nanoparticles coated with CTAB also showed a decrease slightly at 710 nm but improved absorption from 400 nm onwards. In Fig. 12, the average absorption of nanoparticles in the region of 800 to 200 nm is compared. Fe3O4@POE nanoparticles with 98.03% and then Fe_3O_4@SDS and Fe_3O_4@PVP nanoparticles with 95.39% and 95.34% adsorption, respectively, had the highest efficiency.

Nanoparticles coated in alkaline medium by stearic and palmitic had the lowest adsorption with 53.74 and 46.69 %, respectively. This experiment was also repeated by nanoparticles coated with palmitic acid, sodium dodecyl sulfate, polyoxyethylene and polyvinyl pyrrolidone in the amounts of 0.1 and 0.025 g, without the use of an ultrasonic bath.

Table 2 shows the results of the UV-Vis spectroscopy analysis of the crude-solvent emulsions based on a standard solution of 100 mg/L crude oil solutions successively and in triplicate each solution was analyzed on a UV-Vis spectrophotometer with reference to the Soret band appearing at 458 nm.

Table 2. Demulsification results of crude oil-in-water emulsion by nanoparticles coated with fatty acids and surfactants.

Sample	Coating of nanoparticles	The amount of organic matter used for the coating	Absorption, %
1		0.025 g	51.83
2	Palmitic acid	0.05 g	76.60
3		0.1 g	59.23
4	Alkaline Palmitic acid	0.05 g	46.58
5	Oleic acid	0.05 g	74.46
6	Alkaline Oleic acid	0.05 g	91.48
7	Stearic acid	0.05 g	61.7
8	Alkaline Stearic acid	0.05 g	43.74
9		0.025 g	60.45
10	Sodium dodecyl sulfate	0.05 g	93.90
11		0.1 g	78.07
12		0.025 g	69.48
13	Polyoxyethylene	0.05 g	98.13
14		0.1 g	99.71
15		0.025 g	90.32
16	Polyvinylpyrrolidone	0.05 g	94.44
17		0.1 g	95.33
18	Cetyltrimethylammonium bromide	0.05 g	89.36

4. Conclusions

In this study, the iron nanoparticles were coated with the fatty acids and surfactants in order to adsorb the crude oil from water. According to the findings, the best performance is related to nanoparticles with neutral

surfactant coatings such as POE and PVP and nanoparticles with CTAB coating which is a cationic surfactant compared with the nanoparticles with SDS coating which is an anionic surfactant. In the case of nanoparticles coated with smaller fatty acid chain, better adsorption was reported. Palmitic acid with chemical formula $C_{16}H_{32}O_2$ absorbed about 84%, while adsorption by oleic acid with chemical formula $C_{18}H_{34}O_2$ was decreased to 81% and in the case of stearic acid with chemical formula, $C_{18}H_{36}O_2$, the adsorption was reduced to 75%. Another point is that the alkalinization of the medium while coating the nanoparticles with fatty acid has increased only the efficiency in the case of oleic acid while the efficiency was reduced significantly in the case of palmitic and stearic compared to the neutral state. It can be said that the reason for this behavior is that the unsaturation of oleic acid, due to the Van der Waals attraction between the two bonds, the two molecules of oleic acid are conversely connected and the coating density on the nanoparticle surface increases, because the peak intensity of hydroxyl groups is reduced. In the case of palmitic and stearic acids, since in the spectra of nanoparticles coated in the alkaline medium, the intensity of the peaks related to the hydroxyl group and Fe-O bonds increases, the alkaline medium reduces the fatty acids on the nanoparticle surface while the number of hydroxyl groups increases on the surface of nanoparticles.

Author Contributions

Farhatsadat Meibodi: Designing the project, Supervisor
Ebrahim Soori: Performing the experiments

Conflict of Interest

The authors do not have any conflict of interest.

Acknowledgement

We are grateful to Razi University, Kermanshah, Iran, for the financial support of this work.

Data Availability Statement

Data will be made available on request.

References

Adschiri, T. and Yoko, A. (2018) 'Supercritical fluids for nanotechnology', *Journal of Supercritical Fluids*, 134, pp. 167–175. doi: https://doi.org/10.1016/j.supflu.2017.12.033

Akbarzadeh, A., Samiei, M. and Davaran, S. (2012) 'Magnetic nanoparticles: Preparation, physical properties, and applications in biomedicine', *Nanoscale Research Letters*, 7. doi: https://doi.org/10.1186/1556-276X-7-144

Ali, A. *et al.* (2016) 'Synthesis, characterization, applications, and challenges of iron oxide nanoparticles', *Nanotechnology, Science and Applications*, pp. 49–67. doi: https://doi.org/10.2147/NSA.S99986

Arsalani, S. *et al.* (2019) 'Magnetic Fe3O4 nanoparticles coated by natural rubber latex as MRI contrast agent', *Journal of Magnetism and Magnetic Materials*, 475, pp. 458–464. doi: https://doi.org/10.1016/j.jmmm.2018.11.132

Bagwe, R. P., Hilliard, L. R. and Tan, W. (2006) 'Surface modification of silica nanoparticles to reduce aggregation and nonspecific binding', *Langmuir*, 22(9), pp. https://doi.org/4357–4362. doi: 10.1021/la052797j

Ban, Z. *et al.* (2005) 'The synthesis of core-shell iron@gold nanoparticles and their characterization', *Journal of Materials Chemistry*, 15(43), pp. 4660–4662. doi: https://doi.org/10.1039/b504304b

Chicarelli, M. I. *et al.* (1990) 'Application of inductively coupled plasma-mass spectrometry in the detection of organometallic compounds in chromatographic fractions from organic rich shales', *Organic Geochemistry*, 15(3), pp. 267–274. doi: https://doi.org/10.1016/0146-6380(90)90004-J

Colson, P., Henrist, C. and Cloots, R. (2013) 'Nanosphere lithography: A powerful method for the controlled manufacturing of nanomaterials', *Journal of Nanomaterials*. doi: https://doi.org/10.1155/2013/948510

Cosgrove, T. (2009) *Colloid science: principles, methods and applications*, *colloid science: Principles, methods and applications*. 2nd edn. Wiley-Blackwell.

Costa, C. *et al.* (2019) 'Emulsion formation and stabilization by biomolecules: The leading role of cellulose', *Polymers*. doi: https://doi.org/10.3390/polym11101570

Cui, F. *et al.* (2020) 'Oil droplet dispersion under a deep-water plunging breaker: Experimental measurement and numerical modeling', *Journal of Marine Science and Engineering*, 8(4). doi: https://doi.org/10.3390/JMSE8040230

Essien, O. and John, I. (2011) 'Impact of crude-oil spillage pollution and chemical remediation on agricultural soil properties and crop growth', *Journal of Applied Sciences and Environmental Management*, 14(4). doi: https://doi.org/10.4314/jasem.v14i4.63304

Ganapathe, L. S. *et al.* (2020) 'Magnetite (Fe_3O_4) nanoparticles in biomedical application: From synthesis to surface functionalisation', *Magnetochemistry*, pp. 1–35. doi: https://doi.org/10.3390/magnetochemistry6040068

Garcés-Pineda, F. A. *et al.* (2019) 'Direct magnetic enhancement of electrocatalytic water oxidation in alkaline media', *Nature Energy*, 4(6), pp. 519–525. doi: https://doi.org/10.1038/s41560-019-0404-4

Grammatikopoulos, P. *et al.* (2016) 'Nanoparticle design by gas-phase synthesis', *Advances in Physics: X*, pp. 81–100. doi: https://doi.org/10.1080/23746149.2016.1142829

Han, D. *et al.* (2016) 'Synthesis of Fe_3O_4 nanoparticles via chemical coprecipitation method: Modification of surface with sodium dodecyl sulfate and biocompatibility study', *Nanoscience and Nanotechnology Letters*, 8(4), pp. 335–339. doi: https://doi.org/10.1166/nnl.2016.2133

Han, M. *et al.* (2019) 'Research Progress and prospects of marine Oily wastewater treatment: A review', *Water (Switzerland)*. doi: https://doi.org/10.3390/w11122517

Hong, L. *et al.* (2012) 'One-step formation of W/O/W multiple emulsions stabilized by single amphiphilic block copolymers', *Langmuir*, 28(5), pp. 2332–2336. doi: https://doi.org/10.1021/la205108w

Issa, B. *et al.* (2013) 'Magnetic nanoparticles: Surface effects and properties related to biomedicine applications', *International Journal of Molecular Sciences*, pp. 21266–21305. doi: https://doi.org/10.3390/ijms141121266

Jiao, J. *et al.* (1996) 'Preparation and properties of ferromagnetic carbon-coated Fe, Co, and Ni nanoparticles', *Journal of Applied Physics*, 80(1), pp. 103–108. doi: https://doi.org/10.1063/1.362765

Jose, J. *et al.* (2020) 'Magnetic nanoparticles for hyperthermia in cancer treatment: an emerging tool', *Environmental Science and Pollution Research*, 27(16), pp. 19214–19225. doi: https://doi.org/10.1007/s11356-019-07231-2

Kafrouni, L. and Savadogo, O. (2016) 'Recent progress on magnetic nanoparticles for magnetic hyperthermia', *Progress in Biomaterials*, pp. 147–160. doi: https://doi.org/10.1007/s40204-016-0054-6

Khamis, E. A., Hamdy, A. and Morsi, R. E. (2018) 'Magnetite nanoparticles/polyvinyl pyrrolidone stabilized system for corrosion inhibition of carbon steel', *Egyptian Journal of Petroleum*, 27(4), pp. 919–926. doi: https://doi.org/10.1016/j.ejpe.2018.02.001

Lu, F. and Astruc, D. (2018) 'Nanomaterials for removal of toxic elements from water', *Coordination Chemistry Reviews*, pp. 147–164. doi: https://doi.org/10.1016/j.ccr.2017.11.003

M. Alzahrani, A. and Rajendran, P. (2019) 'Petroleum hydrocarbon and living organisms', in *Hydrocarbon Pollution and its Effect on the Environment*. IntechOpen. doi: https://doi.org/10.5772/intechopen.86948

Mahmoudi Saber, M. (2019) 'Strategies for surface modification of gelatin-based nanoparticles', *Colloids and Surfaces B: Biointerfaces*. doi: https://doi.org/10.1016/j.colsurfb.2019.110407

Mamani, J. B. *et al.* (2013) 'Synthesis and characterization of magnetite nanoparticles coated with lauric acid', *Materials Characterization*, 81, pp. 28–36. doi: https://doi.org/10.1016/j.matchar.2013.04.001

Marín, T. *et al.* (2016) 'Influence of surface treatment on magnetic

properties of Fe3O4 nanoparticles synthesized by electrochemical method', *Journal of Physical Chemistry B*, 120(27), pp. 6634–6645. doi: https://doi.org/10.1021/acs.jpcb.6b01796

Masina, N. *et al.* (2017) 'A review of the chemical modification techniques of starch', *Carbohydrate Polymers*, pp. 1226–1236. doi: https://doi.org/10.1016/j.carbpol.2016.09.094

Nobs, L. *et al.* (2003) 'Surface modification of poly(lactic acid) nanoparticles by covalent attachment of thiol groups by means of three methods', *International Journal of Pharmaceutics*. doi: https://doi.org/10.1016/S0378-5173(02)00542-2

Nunes, R. *et al.* (2018) 'Surface modification with polyethylene glycol enhances colorectal distribution and retention of nanoparticles', *European Journal of Pharmaceutics and Biopharmaceutics*, 130, pp. 200–206. doi: https://doi.org/10.1016/j.ejpb.2018.06.029

Ong, H. T., Suppiah, D. D. and Muhd Julkapli, N. (2020) 'Fatty acid coated iron oxide nanoparticle: Effect on stability, particle size and magnetic properties', *Colloids and Surfaces A: Physicochemical and Engineering Aspects*, 125371. doi: https://doi.org/10.1016/j.colsurfa.2020.125371

Onwurah, I. N. E. *et al.* (2007) 'Crude oils spills in the environment, effects and some innovative clean-up biotechnologies', *International Journal of Environmental Research*, pp. 307–320. https://doi.org.10.22059/IJER.2010.142

Ozkaya, T. *et al.* (2009) 'Synthesis of Co3O4 nanoparticles by oxidation-reduction method and its magnetic characterization', *Central European Journal of Chemistry*, 7(3), pp. 410–414. doi: https://doi.org/10.2478/s11532-009-0012-4

Park, J. I. and Cheon, J. (2001) 'Synthesis of "solid solution" and "core-shell" type cobalt-platinum magnetic nanoparticles via transmetalation reactions', *Journal of the American Chemical Society*, 123(24), pp. 5743–5746. doi: https://doi.org/10.1021/ja0156340

Prathna, T. C. *et al.* (2011) 'Biomimetic synthesis of silver nanoparticles by Citrus limon (lemon) aqueous extract and theoretical prediction of particle size', *Colloids and Surfaces B: Biointerfaces*, 82(1), pp. 152–159. doi: https://doi.org/10.1016/j.colsurfb.2010.08.036

Salunkhe, A. B. *et al.* (2013) 'Polyvinyl alcohol functionalized cobalt ferrite nanoparticles for biomedical applications', *Applied Surface Science*, 264, pp. 598–604. doi: https://doi.org/10.1016/j.apsusc.2012.10.073

Shamim, A. *et al.* (2018) 'Synthesis of metallic nanoparticles by physical, chemical and biological methods and their characterization'. Available at: http://uow.edu.pk/ORIC/Publications/4th MDSRIC-296.pdf (Accessed: 1 July 2023).

Takai, Z. I. *et al.* (2019) 'Preparation and characterization of magnetite (Fe3O4) nanoparticles by sol-gel method', *International Journal of Nanoelectronics and Materials*, 12(1), pp. 37–46. http://eprints.uthm.edu.my/id/eprint/4108

Tassa, C., Shaw, S. Y. and Weissleder, R. (2011) 'Dextran-coated iron oxide nanoparticles: A versatile platform for targeted molecular imaging, molecular diagnostics, and therapy', *Accounts of Chemical Research*, pp. 842–852. doi: https://doi.org/10.1021/ar200084x

Thompson, D. A. and Best, J. S. (2000) 'Future of magnetic data storage technology', *IBM Journal of Research and Development*, 44(3), pp. 311–322. doi: https://doi.org/10.1147/rd.443.0311

Venkataraman, N. V. and Vasudevan, S. (2001) 'Conformation of methylene chains in an intercalated surfactant bilayer', *Journal of Physical Chemistry B*, 105(9), pp. 1805–1812. doi: https://doi.org/10.1021/jp002505h

Vidal, L. *et al.* (2008) 'Chemically surface-modified carbon nanoparticle carrier for phenolic pollutants: Extraction and electrochemical determination of benzophenone-3 and triclosan', *Analytica Chimica Acta*, 616(1), pp. 28–35. doi: https://doi.org/10.1016/j.aca.2008.04.011

Wang, H. *et al.* (2015) 'Acid-functionalized magnetic nanoparticle as heterogeneous catalysts for biodiesel synthesis', *Journal of Physical Chemistry C*, 119(46), pp. 26020–26028. doi: https://doi.org/10.1021/acs.jpcc.5b08743

Yu, S. *et al.* (2019) 'Chitosan and chitosan coating nanoparticles for the treatment of brain disease', *International Journal of Pharmaceutics*, 560, pp. 282–293. doi: https://doi.org/10.1016/j.ijpharm.2019.02.012

Zhu, N. *et al.* (2018) 'Surface modification of magnetic iron oxide nanoparticles', *Nanomaterials*. doi: https://doi.org/10.3390/nano8100810